Philosophical Magazine Letters,
Vol. 86, No. 1, January 2006, 5–11

Taylor & Francis
Taylor & Francis Group

Ni-based fully amorphous metallic coating with high corrosion resistance

A. P. WANG†, T. ZHANG‡ and J. Q. WANG*†

†Shenyang National Laboratory for Materials Science, Institute of Metal Research, CAS, Shenyang 110016, China
‡State Key Laboratory for Corrosion and Protection, Institute of Metal Research, CAS, Shenyang 110016, China

(*Received 24 July 2005; in final form 9 October 2005*)

A $Ni_{53}Nb_{20}Ti_{10}Zr_8Co_6Cu_3$ fully amorphous metallic coating has been deposited by means of kinetic metallization (KM) using gas atomized powders. As the thickness of the amorphous metallic coating is increased to 400 μm, it attains the excellent corrosion resistance of the amorphous alloy, as indicated by the extremely low passive current density and wide passive region in 1 kmol/m^3 HCl aqueous solution. The corrosion rate is as low as 10^{-3} mm/year in the extremely corrosive environment of 6 kmol/m^3 HCl aqueous solution.

1. Introduction

During the last few decades, there has been considerable interest in the corrosion resistance of amorphous alloys. Their high corrosion resistance exists in a broad range of aqueous environments owing to the easy formation of a protective oxide layer at the surface, making them well suited for use as coatings to withstand aggressive environments [1, 2].

Thermal spraying is one of the techniques for fabricating amorphous metallic coatings [3, 4]. Because crystallization and oxidation often occur during thermal spraying of amorphous powders, it is very difficult to obtain fully amorphous metallic coatings. As a result, the coatings are partially amorphous and have reduced corrosion resistance compared to the corresponding amorphous alloys [3].

Kinetic metallization (KM) is a newly developed process [5]. It is a low-temperature spraying process and uses helium gas to feed and accelerate the powders. As the temperature of the amorphous powders, heated in the spraying process, is lower than that of glass transition of the amorphous alloy and no oxidation atmosphere exists in the spraying environment, crystallization and oxidation of the sprayed amorphous powders are avoided. The amorphous structure of the powders is retained when they are consolidated to form the coating. In this sense, KM is an ideal process to fabricate fully amorphous metallic coatings.

*Corresponding author. Email: jqwang@imr.ac.cn

Philosophical Magazine Letters
ISSN 0950-0839 print/ISSN 1362-3036 online © 2006 Taylor & Francis
http://www.tandf.co.uk/journals
DOI: 10.1080/09500830500479718

Nickel-based alloys are very important materials for industrial applications. However, it is difficult to produce Ni-based bulk metallic glasses. The best glass forming ability (GFA) achieved so far in Ni-based systems corresponds to a limiting amorphous thickness of 3–5 mm [6–8]. In this work, a $Ni_{53}Nb_{20}Ti_{10}Zr_8Co_6Cu_3$ (at.%) alloy, which has a limiting amorphous thickness of ~3 mm, was adopted to produce amorphous metallic coatings by KM spraying.

2. Experimental

A $Ni_{53}Nb_{20}Ti_{10}Zr_8Co_6Cu_3$ (at.%) master alloy was prepared by induction-melting of high-purity elemental constituents (Ni: 99.9%, Nb: 99.7%, Ti: 99.9%, Zr: 99.8%, Co: 99.9%, Cu: 99.999%) in a yttria-stabilized zirconia crucible under an argon atmosphere. The alloy powders were produced by high-pressure Ar gas atomization. The atomized powders were sieved according to conventional sieve analysis and divided into different size ranges. A SEM micrograph of the as-atomized powders with particle sizes below 25 μm, which were used for the KM spraying, is shown in figure 1. It can be seen that most of the particles have a near-spherical form. The details of the KM process have been described elsewhere [5]. Briefly, the amorphous alloy powders were sprayed by preheated helium (~570 K and 90 psi) through a specially designed sonic deposition nozzle that accelerates the metal particles entrained in the carrier gas. Once accelerated to a high speed (750–900 m/s), the particles are directed onto the low-carbon-steel substrate, producing a coating. As higher spray temperature and deposition efficiency can lead to an effective softening and a larger strain of the sprayed particles, optimized parameters with a spray temperature of ~570 K and a deposition efficiency of ~40% were used to prepare the amorphous metallic coating.

The microstructure of the atomized powders and as-deposited coatings was characterized using X-ray diffraction (XRD) (Rigaku D/max 2400) with Cu Kα radiation, scanning electron microscopy (SEM) (JMS-6301) and transmission electron microscopy (TEM) (JEM-2000FXII). The samples were cut from the deposited coatings by electro-spark discharge, mechanically ground and, then,

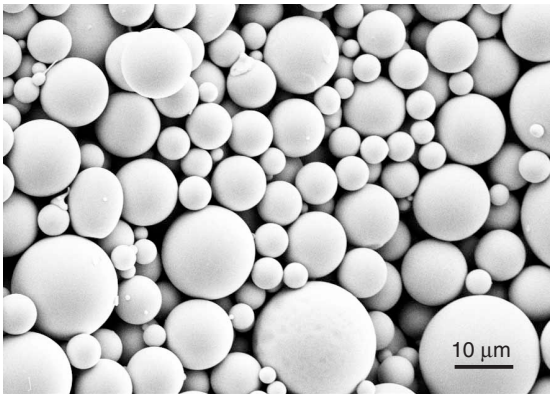

Figure 1. SEM micrograph of the as-atomized powders with particle sizes below 25 μm.

crushed for XRD experiment or thinned by ion milling to produce thin foil specimens for TEM observations. The thermal stability of the atomized powders was examined using differential scanning calorimeter (DSC) (Perkin–Elmer DSC-7) in a continuous heating mode at a rate of 0.33 K/s.

The corrosion property of the coatings was evaluated by electrochemical measurement using a potentiostat/galvanostat (EG&G Princeton Applied Research Model 273). Electrochemical measurement was conducted in a three-electrode cell using a platinum counter electrode and an Ag/AgCl reference electrode. Potentiodynamic polarization curves were measured with a potential sweep rate of 0.33 mV/s in an aqueous solution open to air at 298 K after immersing the samples for several minutes, when the open-circuit potential became almost steady. The corrosion rate was estimated from the weight loss after immersion in 6 kmol/m^3 HCl solution open to air at 298 K for 100 h.

3. Results and discussion

The XRD pattern shown in figure 2a indicates complete glass formation of the gas atomized NiNbTiZrCoCu powders with a size range of below 63 μm. This wide size range of atomized amorphous powders arises from the limiting amorphous thickness of ~3 mm of the Ni-based alloy. The glass transition temperature of the sprayed amorphous powders is about 826 K from the DSC trace in figure 2b, which is much higher than the temperature (~570 K) of powders heated by the hot carrier gas in the KM process. Crystallization of the amorphous powders is thus avoided. Oxidation is also prevented as the inert He is used as the powders feed gas and accelerating gas. The sprayed powders would be expected to retain the amorphous structure in the coating. The XRD pattern of the coatings given

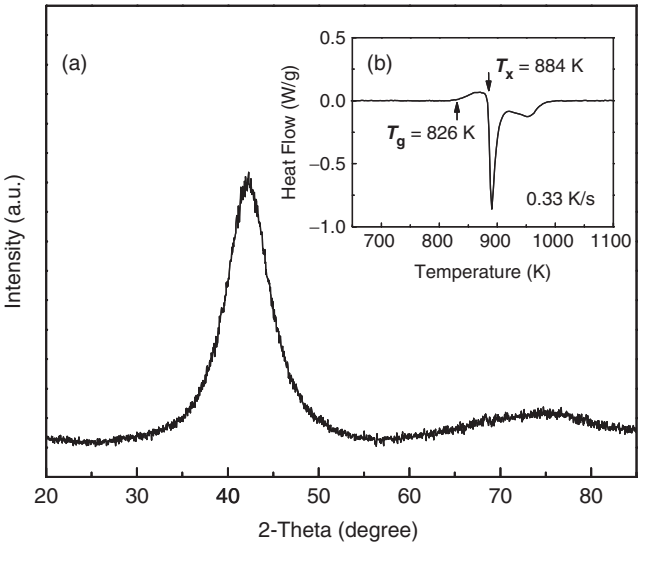

Figure 2. (a) XRD pattern of the gas-atomized powders with diameters <63 μm. (b) DSC trace of the powders with diameters <25 μm.

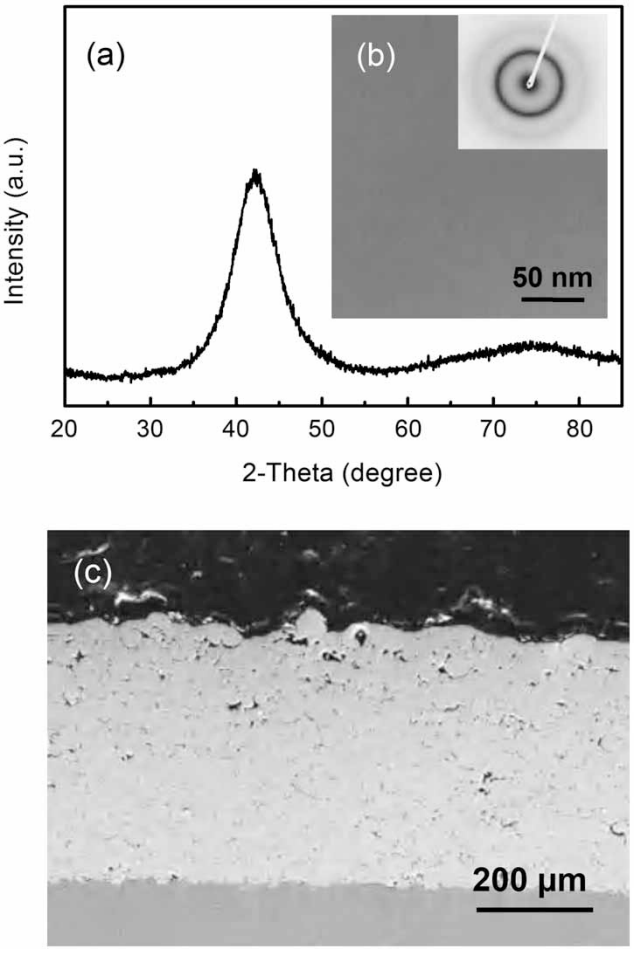

Figure 3. (a) XRD pattern of the KM-sprayed coating. (b) Dark-field TEM image and selected area electron diffraction (SAED) of a 400 μm coating, taken from a region ~200 μm from the top. (c) SEM image of a cross-section of the as-sprayed coating.

in figure 3a confirms this suggestion: only a broad halo is present, indicating an entirely amorphous phase formation. The TEM image of the coating in figure 3b confirms again the complete glass formation. A SEM image of a typical region from the cross-section of a coating with a thickness of 400 μm is shown in figure 3c. It generally has a featureless structure except some pores, which appear as very dark contrast regions.

Figure 4a shows potentiodynamic polarization curves of some Ni-based, Fe-based amorphous ribbons, Zr-based bulk amorphous strip and two traditional materials of electroplated-Cr and stainless steel in 1 kmol/m^3 HCl aqueous solution. The NiNbTiZrCoCu amorphous alloy exhibits the lowest passive current density and widest passive region, which indicate its high corrosion resistance in this aggressive solution. Figure 4b shows the potentiodynamic polarization curves of the coatings with different thickness, in comparison with the corresponding amorphous ribbon and stainless-steel substrate in 1 kmol/m^3 HCl aqueous solution.

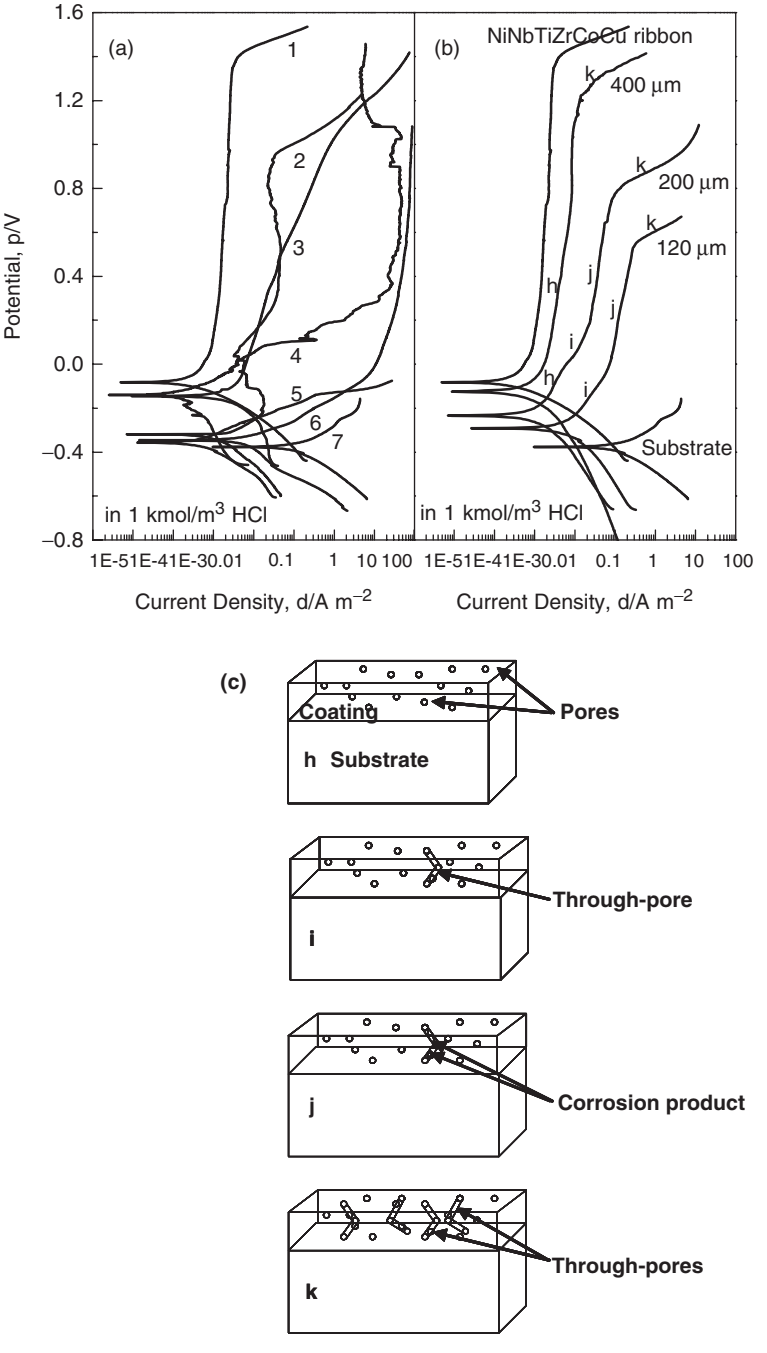

Figure 4. (a) Potentiodynamic polarization curves of the amorphous $Ni_{53}Nb_{20}Ti_{10}Zr_8Co_6Cu_3$ (1), $Fe_{43}Cr_{16}Mo_{16}(C,B,P)_{25}$ (2), $Ni_{65}Nb_5Cr_5Mo_5P_{14}B_6$ (3), $Ni_{59}Zr_{20}Ti_{16}Si_2Sn_3$ (4), $Zr_{55}Al_{10}Cu_{30}Ni_5$ (5), alloys, electroplated-Cr (6), 1Cr18Ni9Ti stainless steel (7), in 1 kmol/m^3 HCl aqueous solution. (b) Potentiodynamic polarization curves of the coatings with different thickness of 120, 200 and 400 μm, compared with those of NiNbTiZrCoCu amorphous ribbon and stainless steel substrate in 1 kmol/m^3 HCl aqueous solution. (c) A sketch of the evolution of through-pores. The schematic structures *h–k* correspond to the positions *h–k* in the curves (b).

It was found that the corrosion resistance of the coatings increases with their thickness. When the thickness of the amorphous metallic coatings is increased from 120 to 400 μm, the coatings gradually approach the very high corrosion resistance of the NiNbTiZrCoCu amorphous alloy, as indicated by the extremely low passive current density and wide passive region.

It is well known that anticorrosion coating must be impermeable to protect the substrate. The presence of through-pores can provide a passage for substrate to react chemically or electrochemically with a corrosive environment, leading to electrochemical dissolution of the substrate. A through-pore is formed by individual pores connecting with each other along the thickness of the coating, but there is no suitable method to measure accurately the through-pore, which depends on the coating stack structure and thickness [9, 10]. The porosities of the KM coatings with different thickness from 120 to 400 μm measured by image analysis were almost the same ($\bar{P} = 2.30 \pm 0.14\%$). It is expected that the through-pores are more difficult to form with increased thickness of the coating, which is reflected in the polarization curves of KM coatings in figure 4b. The coating with a thickness of 200 μm has a typical polarization curve, which can be divided into four stages above the equilibrium corrosive potential. The curve exhibits passivation in stage *h* just like the corresponding amorphous alloy; then active dissolution occurs in stage *i* owing to the formation of through-pore in the coating with increased potential. After that, passivation sets in stage *j* because the through-pore is jammed with the corrosion product of the substrate. Finally, active dissolution occurs again in stage *k* on account of the dissolution of the corrosion product in the through-pores and the formation of more through-pores with enhanced potential, leading to fast dissolution of the substrate. This model can be seen in figure 4c. With the thickness of the coating decreased to 120 μm, the formation of through-pore is easier, requiring only the equilibrium corrosive potential and the polarization curve just exhibits

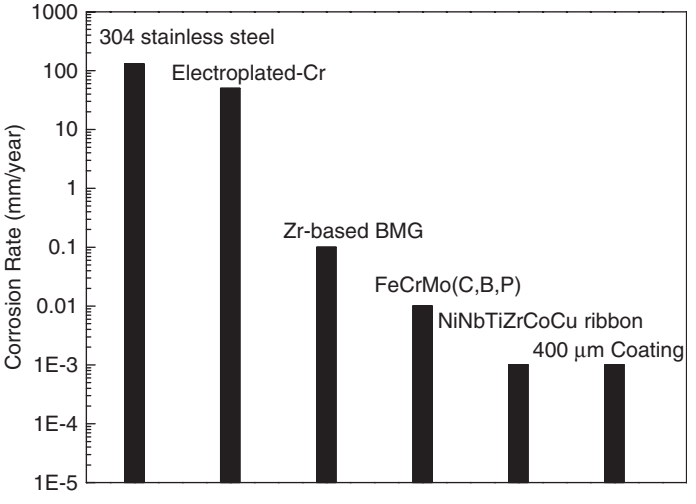

Figure 5. Corrosion rate comparison of type 304 stainless steel [12], electroplated-Cr [12], Zr-based BMG [2], amorphous FeCrMo(C,B,P) [11], the KM NiNbTiZrCoCu coating with thickness of 400 μm and the corresponding amorphous ribbon in 6 kmol/m^3 HCl aqueous solution by immersion test.

stages *i*, *j* and *k*. However, with the thickness of the coating increased to 400 μm, through-pore is very difficult to form and the passivation (stage *h*) of the polarization curve is extended to very high potential.

Further characterization of the corrosion resistance of the coating was performed by an immersion test in 6 kmol/m^3 HCl aqueous solution. The result is displayed in figure 5. The corrosion rate of the coating with thickness 400 μm has almost the same value as that of the corresponding NiNbTiZrCoCu amorphous alloy. They have a lower corrosion rate, about 10^{-3}mm/year, when compared with some of typical Fe-based [11], Zr-based amorphous alloys [2] and the electroplated-Cr and stainless steel [12]. This very low corrosion rate makes the Ni-based fully amorphous metallic coating a good candidate for anticorrosion applications.

4. Conclusions

A Ni-based fully amorphous metallic coating was obtained by KM spraying of amorphous powders. The corrosion resistance of the coating is related to the through-porosity, which depends on the coating thickness. A coating with a thickness of 400 μm nearly reaches the same high corrosion resistance as that of the NiNbTiZrCoCu amorphous alloy, in the extremely corrosive environment of 6 kmol/m^3 HCl aqueous solution. This excellent corrosion resistance opens opportunities for anticorrosion applications to withstand aggressive environments.

Acknowledgements

This work was supported by the National Natural Science Foundation of China (grant nos. 50271070 and 50323009). Thanks are due to Professor E. Ma and Dr Y. Li for helpful discussions. The authors are also with the MANS research team, supported by the Chinese Academy of Sciences.

References

[1] A.L. Greer, K.L. Rutherford and I.M. Hutchings, Inter. Mater. Rev. **47** 87 (2002).
[2] D. Zander and U. Köster, Mater. Sci. Eng. A **375/377** 53 (2004).
[3] A.P. Wang, T. Zhang and J.Q. Wang, Mater. Trans. **46** 1010 (2005).
[4] H.J. Kim, K.M. Lim, B.G. Seong, *et al.*, J. Mater. Sci. **36** 49 (2001).
[5] H. Gabal, Adv. Mater. Process. **47** (2004).
[6] T. Zhang and A. Inoue, Mater. Trans. **43** 708 (2002).
[7] J.K. Lee, D.H. Bae, S. Yi, *et al.*, J. Non-Cryst. Solids **333** 212 (2004).
[8] D.H. Xu, G. Duan, W.L. Johnson, *et al.*, Acta Mater. **52** 3493 (2004).
[9] J. Kawakita, S. Kuroda and T. Kodama, Surf. Coat. Technol. **166** 17 (2003).
[10] S.H. Ahn, J.H. Lee, H.G. Kim, *et al.*, Appl. Surf. Sci. **233** 105 (2004).
[11] S.J. Pang, T. Zhang, K. Asami, *et al.*, Corros. Sci. **44** 1847 (2002).
[12] X.Y. Li, E. Akiyama, H. Habazaki, *et al.*, Corros. Sci. **41** 1095 (1999).